

Ultrasonic study of the charge-stripe phase in $\text{La}_{1.88-y}\text{Nd}_y\text{Sr}_{0.12}\text{CuO}_4$

J. F. Qu, Y. Liu, F. Wang, X. Q. Xu, and X. G. Li*

Hefei National Laboratory for Physical Sciences at Microscale, Department of Materials Science and Engineering,
University of Science and Technology of China, Anhui, Hefei 230026, China

and International Center for Materials Physics, Academia Sinica, Shenyang 110015, China

(Received 29 March 2004; revised manuscript received 28 June 2004; published 4 March 2005)

Elastic energy loss spectra for $\text{La}_{1.88-y}\text{Nd}_y\text{Sr}_{0.12}\text{CuO}_4$ (LNSCO) polycrystalline samples ($y=0, 0.20, 0.30, 0.40, 0.50, 0.60$) show a transformation of charge stripes from dynamic to static state. A sharp peak P_1 in energy loss spectrum around 70 K observed for $y \geq 0.3$ samples indicates the formation of static stripe order, and a relative stiffening of the sound velocity below P_1 temperature suggests the development of the static charge stripes. Both the intensity of P_1 and the relative stiffening of the velocity increase with increasing Nd doping due to the stabilization of the static charge stripes. The evolution of another new broad peak P_2 observed around 100 K, which has never been reported for the system before, is consistent with the scenario of interaction between dynamic charge strips and pinning centers. The activation energy of the charge stripes overcoming the pinning centers was suggested to increase with increasing Nd doping.

DOI: 10.1103/PhysRevB.71.094503

PACS number(s): 74.72.Dn, 74.62.Dh, 74.25.Ld

I. INTRODUCTION

There is growing evidence that charges and spins self-organize in CuO_2 planes in a peculiar striped manner at least in some high- T_c cuprates, where the doped holes are arranged in one-dimensional (1D) lines, “charge stripes” that separate the antiferromagnetic domains.¹⁻⁴ Experimentally, Nd-doped $\text{La}_{2-x}\text{Sr}_x\text{CuO}_4$ (LSCO) has attracted much attention since the discovery of the static charge stripe order by Tranquada *et al.*²⁻⁴ The incommensurate, *inelastic* magnetic peak found in the LSCO system⁵ in *inelastic* neutron scattering, which has been attributed to the existence of charge stripes in a fluctuating sense, has also become the most interesting hot topic in the field. Lots of experiments have demonstrated that both dynamic and static charge stripes play an important role in many unusual properties of cuprates.⁶⁻¹⁰ But study on the dynamics of charge stripes is still quite scarce.

An interesting question arises from how the dynamic charge stripes interact with the crystal lattice and how they transform to static ones. Up to date, the dynamic process of such a transformation has never been observed experimentally. Recently, a relaxation process in the elastic energy loss spectrum of $\text{La}_{2-x}\text{Sr}_x\text{CuO}_4$ at a measuring frequency of ~ 1 kHz showed that the energy loss peak around 80 K shifts to higher temperature at higher measuring frequency, and disappears in the overdoped state $x=0.20$, identified with the scenario of the interaction between disordered dynamic charge stripes and pinning centers induced by Sr dopants.¹¹ With a higher measuring frequency (\sim MHz) than the internal friction spectroscopy, the ultrasonic attenuation technique is also a sensitive tool for studying low-energy dynamics of the crystal lattice. The technique had been used to study the elastic properties extensively for both the bulk and single-crystalline materials of high- T_c superconductivity,¹²⁻¹⁷ especially for the relation between superconductivity and structural instability for LSCO system.¹⁴ Since the charge stripes tend to produce a structure distortion¹⁸ and the motion of

them acting as a line defect of electromagnetic structure is coupled with the crystal lattice, the ultrasonic attenuation measurement will be useful to investigate the existence and the motion of charge stripes.

Considering the difference of the frequency used in the two techniques (\sim kHz for internal friction spectroscopy, while \sim MHz for ultrasonic attenuation measurement), the relaxation process found by Cardero *et al.*¹¹ should be observed at a higher temperature in ultrasonic attenuation measurements. Motivated by the proposal, we have carried out systematic ultrasonic attenuation measurements on the $\text{La}_{1.88-y}\text{Nd}_y\text{Sr}_{0.12}\text{CuO}_4$ (LNSCO) series in the present work. Here, the advantage of studying Nd-doped LSCO is that they can give information not only for the dynamic charge stripes but also for the static ones. The experimental results depict that with increasing Nd-doping level, the dynamic charge stripes were pinned down gradually and the static ones become more and more stable. A new energy loss peak observed around 100 K has been attributed to the interaction between dynamic charge stripes and pinning centers.

II. EXPERIMENT

The polycrystalline $\text{La}_{2-x}\text{Sr}_x\text{CuO}_4$ ($x=0, 0.03, 0.12, 0.15, 0.19$) and $\text{La}_{1.88-y}\text{Nd}_y\text{Sr}_{0.12}\text{CuO}_4$ ($y=0.20, 0.30, 0.40, 0.50, 0.60$) specimens were synthesized by a standard solid-state reaction. Stoichiometric amounts of high-purity La_2O_3 , Nd_2O_3 , SrCO_3 , and CuO_2 were mixed intimately in an agate mortar and pestle. The reactants were sintered in air at 900, 950, and 1000 °C, respectively, for 20 h with regrinding between firings. Finally, the fired powder were pelleted and fired at temperatures varying from 1050 to 1080 °C for 20 h in flowing oxygen atmosphere according to the doping level x and y .

Powder x-ray diffraction measurements were made on the MXP18AHF powder x-ray diffractometer (MAC Science Co. Ltd., Japan) using a high-intensity $\text{Cu } K\alpha$ ($\lambda = 1.54056 \text{ \AA}$) radiation. The diffraction patterns indicate that

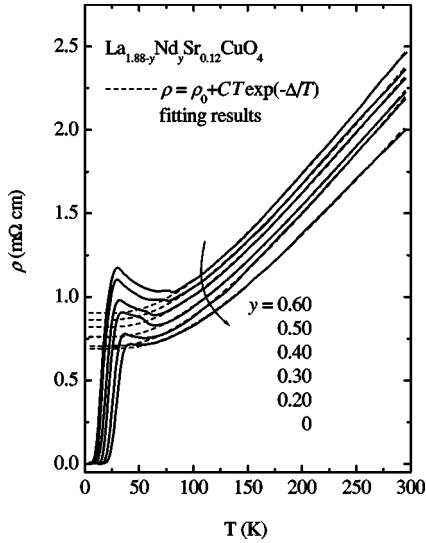


FIG. 1. Temperature dependence of the resistivity ρ for LNSCO ($y=0, 0.20, 0.30, 0.40, 0.50, 0.60$). Between $T_d < T < 300$ K for $y \geq 0.3$ and $T_c < T < 300$ K for $y=0, 0.20$, the resistivity of the samples can be well fitted with Moshchalkov's 1D transport equation (Ref. 23), as shown by dashed lines.

all the samples are crystallized in single phase. The longitudinal ultrasonic attenuation was measured using the digital AUV-100 Advanced Ultrasonic Workstation (Matec Instrument Companies, USA) at temperatures from 20 to 200 K. LiNbO₃ transducers were used for the generation of the 7- and 14-MHz longitudinal ultrasonic. Sound velocity (V) and elastic energy loss (Q^{-1}) were calculated through the following relations, respectively:¹⁹

$$V = 2L/t, \quad (1)$$

$$Q^{-1} = -\ln(A_{n+1}/A_n)/\pi ft, \quad (2)$$

where L is the thickness of the sample, f is measuring frequency, A_{n+1} and A_n are the amplitude of successive pulse echoes, and t is the time difference between them. Resistivity $\rho(T)$ was measured using a standard four-probe technique at temperatures from 4 to 300 K. All data were collected upon warming.

III. RESULTS AND DISCUSSION

Figure 1 shows the temperature dependence of the resistivity of the La_{1.88-y}Nd_ySr_{0.12}CuO₄ system. With increasing Nd doping level y , the room-temperature resistivity increases and the superconductivity is suppressed. The superconducting transition temperature T_c for $y \geq 0.3$ is below 10 K, as reported before.^{20,21}

A little jump of the resistivity ρ for $y \geq 0.3$ at the doping-dependent temperature T_d indicates the low-temperature orthorhombic to low-temperature tetragonal (LTO-LTT) structure phase transition, which is in good agreement with previous results.^{22,23} The interest is focused on the different influence of Nd doping on the behavior of the resistivity in LTO and LTT phases. The resistivity ρ above T_d for all

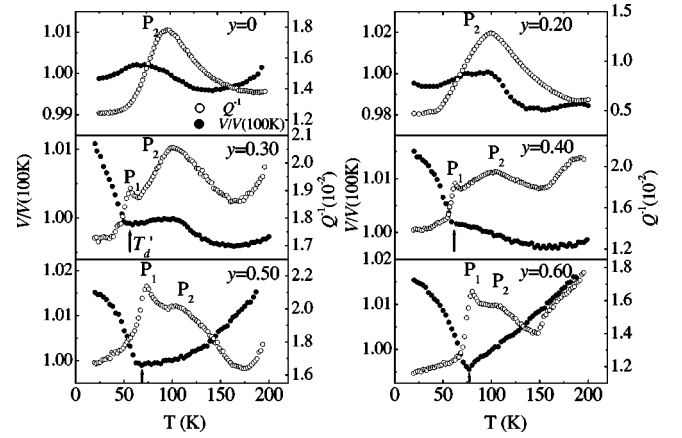


FIG. 2. Temperature dependence of the relative ultrasonic velocity $V/V(100\text{ K})$ (solid circles) and elastic energy loss Q^{-1} (open circles) at a measuring frequency of 7 MHz for La_{1.88-y}Nd_ySr_{0.12}CuO₄ samples ($y=0, 0.20, 0.30, 0.40, 0.50, 0.60$). P_1 and P_2 denote the energy loss peaks around 70 and 100 K, respectively.

LNSCO samples can be well fitted with the 1D transport equation (dashed lines in Fig. 1) proposed by Moshchalkov and co-workers²⁴ as follows:

$$\rho = \rho_0 + CT \exp\left(-\frac{\Delta}{T}\right), \quad (3)$$

where ρ_0 is the residual resistivity, C is a system-dependent constant, and Δ is the spin gap. Below a temperature T^* (empirically expressed as $T^* = 2\Delta$) the dynamic stripe correlations are formed. The similar temperature dependence of the resistivity above T_d indicates that the 1D dynamic-stripe-dominated charge transport is essentially identical for all the LNSCO samples. Below T_d , the static stripe order develops with decreasing temperature.²⁻⁴ The increase of ρ with decreasing temperature discriminates the charge transport of the spin-charge-ordered phase from the normal phase of HTSC. With increasing doping level, the increase of the up turn of the resistivity indicates that the static charge stripe becomes more stable with higher doping level.

It's captivating but has been seldom studied that how the dynamic charge stripes evolve and transform to static ones. To gain insight into the question, we carried out the systematic ultrasonic attenuation measurements on La_{1.88-y}Nd_ySr_{0.12}CuO₄ ($y=0, 0.20, 0.30, 0.40, 0.50, 0.60$) system since both the motion of charge stripes and the formation of static stripe order are coupled with the crystal lattice. The temperature dependences of the sound velocity and the elastic energy loss at a measuring frequency of 7 MHz for the series are presented in Fig. 2. Upon cooling from 200 K, there are two energy loss peaks were observed for the system. One is around 70 K for $y \geq 0.3$, named P_1 , and the other is around 100 K for all the samples, named P_2 . As shown in Fig. 2, with increasing Nd content, P_1 becomes more and more strong and P_2 seems to be ambiguous for $y=0.50$ and 0.60 . Associated with the appearance of P_1 and P_2 , the sound velocity for $y \geq 0.30$ shows an anomalous stiffness below a doping dependence temperature around 70 K,

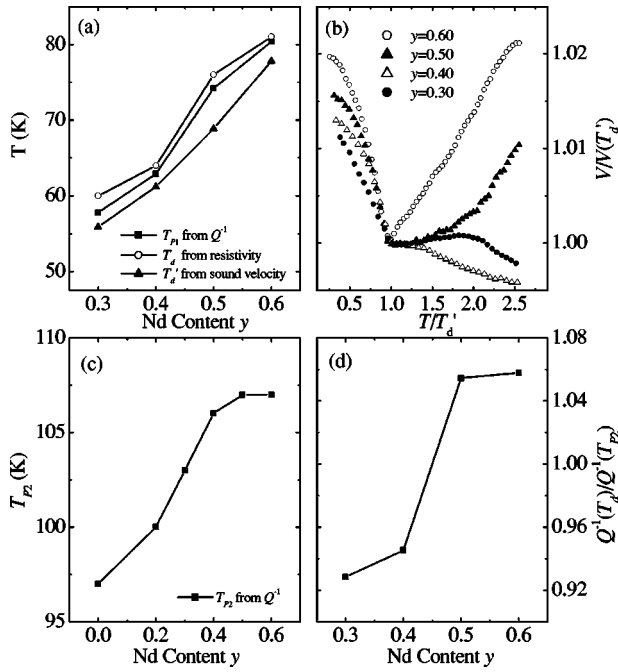


FIG. 3. (a) Nd doping dependence of the LTO-LTT transition temperature T_d determined by resistivity (circles), temperature T_{P_2} of energy loss peak P_2 (squares) and $T_{d'}$ determined by sound velocity (triangles) for LNSCO. (b) Temperature dependence of the relative ultrasonic velocity ($V/V(T_{d'})$) for LNSCO ($y=0.30, 0.40, 0.50, 0.60$). The temperature is normalized to $T/T_{d'}$. (c) Nd doping dependence of T_{P_2} for LNSCO. (d) Nd doping dependence of the peak intensity ratio of P_1 and P_2 in Q^{-1} for LNSCO. The solid lines are guide to the eye.

and for $y=0, 0.20, 0.30$ and 0.40 , the velocity shows small stiffening and forms a step near 100 K.

Figure 3(a) shows the Nd-doping dependence of the P_1 temperature T_{P_1} , the sound velocity stiffening temperature $T_{d'}$ and the LTO-LTT transition temperature T_d measured by resistivity. One can see that T_{P_1} for $y \geq 0.30$ samples is well consistent with T_d which is somewhat higher than $T_{d'}$. Both T_d and $T_{d'}$ increase monotonously with increasing Nd content, and show almost the same doping dependence. Figure 3(b) shows the temperature dependence of the relative velocity for LNSCO with normalized temperature $T/T_{d'}$. It is clear that the anomalous stiffening of the velocity increases with increasing doping level. The P_2 temperature T_{P_2} increases quickly with increasing y for $y < 0.4$, and changes slowly for $y > 0.4$, as shown in Fig. 3(c). Figure 3(d) displays that the intensity ratio $Q^{-1}(T_{d'})/Q^{-1}(T_{P_2})$ increases monotonically with increasing Nd doping level.

It was demonstrated that Nd-doped LSCO undergoes a structure phase transition from a space group $Bmab$ (LTO1 or LTO) to $P4_2/nm$ (LTT) around 70 K with a $Pccn$ [low-temperature orthorhombic 2 (LTO2)] phase intermediate in a wide doping range.^{2,25-27} It is proposed that the peak P_1 accompanied with the anomalous sound velocity stiffening, which was also observed in $\text{La}_{1.875-y}\text{Nd}_y\text{Ba}_{0.125}\text{CuO}_4$ system by another group,¹⁶ can be attributed directly to the LTO-LTT transition. It was widely accepted²⁻⁴ that in LNSCO with carrier concentration near 1/8 the occurrence of the

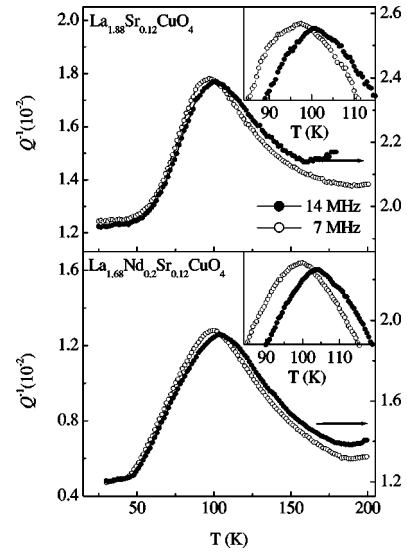


FIG. 4. Elastic energy loss spectrum Q^{-1} for $\text{La}_{1.88}\text{Sr}_{0.12}\text{CuO}_4$ and $\text{La}_{1.68}\text{Nd}_{0.2}\text{Sr}_{0.12}\text{CuO}_4$ samples at measuring frequencies of 7 and 14 MHz. Insets show the magnification of the peak around 100 K.

static stripe order is related to the structure transition from LTO to LTT phase, since the LTT deformation is regarded as a collective pinning potential stabilizing charge stripes, and the onset temperature of static stripe order coincides with T_d . Thus, the appearance of P_1 symbolizes the formation of static charge stripes, and the stiffening of the velocity implies the evolution of the static stripe order. The increases of the temperature and intensity of P_1 with increasing Nd doping indicate that the charge stripes were pinned down to static ones gradually.

Another important result of our ultrasonic attenuation measurements is the characteristic of the new type of elastic energy loss peak P_2 . It should be pointed out that for LNSCO there was no anomaly observed around 100 K by measuring electric and magnetic properties and structure characterization.²⁻⁶ Figure 4 shows the energy loss spectrum of samples $\text{La}_{1.88}\text{Sr}_{0.12}\text{CuO}_4$ and $\text{La}_{1.68}\text{Nd}_{0.2}\text{Sr}_{0.12}\text{CuO}_4$ measured at two different frequencies. It is found that P_2 shifts toward high temperature for about 3–4 K for both samples with increasing frequency from 7 to 14 MHz. The results associated with the step of sound velocity around 100 K demonstrate that P_2 should correspond to a thermally activated relaxation process with the activation energy E/k_B about 1800 K in present samples. [The activation energy for a thermally activated relaxation process can be deduced from the formula $\ln(\omega_2/\omega_1) = E/k_B(T_1^{-1} - T_2^{-1})$, where T_1 and T_2 are the energy loss peak temperatures under frequency $\omega_1/2\pi$ and $\omega_2/2\pi$, respectively.¹⁹] For $y \geq 0.3$ (not shown here), it is difficult to determine the shift of P_2 precisely due to the intervention of P_1 .

Since P_2 appears for $y=0$, one can confirm that P_2 does not originate from Nd doping. The interstitial oxygen cannot be the cause of P_2 either because their mobility is frozen below 140–150 K.²⁸ The maximum of the energy loss at 230 K due to the diffusion of the interstitial oxygen in internal friction spectroscopy²⁹ would shift to a higher tempera-

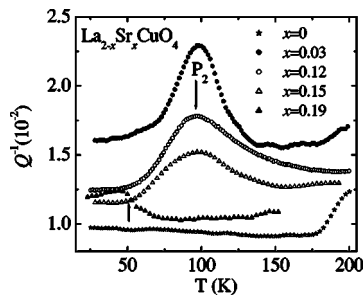


FIG. 5. Elastic energy loss spectrum Q^{-1} for $\text{La}_{2-x}\text{Sr}_x\text{CuO}_4$ samples ($x=0, 0.03, 0.12, 0.15, 0.19$). The arrow around 50 K indicates the HTT-LTO structure phase transition for $x=0.19$.

ture in ultrasonic attenuation measurements and lie out of the temperature window of our experiments. Practically, there was no anomaly identified with the diffusion of the interstitial oxygen below room temperature in previous ultrasonic attenuation measurements for LSCO.^{13,14}

To investigate the origin of P_2 further, we carried out ultrasonic attenuation measurements at frequency of 7 MHz on other four $\text{La}_{2-x}\text{Sr}_x\text{CuO}_4$ samples with $x=0, 0.03, 0.15$, and 0.19 . As shown in Fig. 5, P_2 appears for $x=0.03$ and 0.15 and such a peak disappears for $x=0$ and 0.19 . In addition, a new energy loss peak observed around 50 K for $x=0.19$ sample can be contributed to the high-temperature tetragonal to low-temperature orthorhombic (HTT-LTO) structure phase transition.¹¹ The Sr doping dependence of the intensity of P_2 indicates that it may have something to do with the charge carriers.

An appreciable explanation of the appearance of P_2 comes from the interaction between dynamic charge stripes and pinning centers. Considering that the charge carriers tend to be in a uniform metallic state when x reaches an over doped level,¹ the Sr doping dependence of the intensity of P_2 shown in Fig. 5 suggests that P_2 should correlate with dy-

namic charge stripes. In addition, the activation energy $E/k_B \sim 1800$ K is well consistent with that of charge stripes overcoming pinning centers reported by Cordero *et al.*¹¹ In the simplest picture, irregularities in the ordered pattern of the octahedral tilts induced by Sr and Nd dopants will be the pinning centers for the dynamic charge stripes. Although the charge stripes fluctuate fast far from the pinning centers, the process of the stripes overcoming the pinning centers requires certain activation energy.¹¹ From the Arrhenius law one can deduce that the activation energy is proportional to the peak temperature by supposing that the frequency factor τ_0^{-1} for the dynamic charge stripes is a constant. The increase of T_{P_2} in narrow temperature range suggests that the activation energy increases slightly with increasing Nd content and tends to be saturated in higher doping level. The characteristics of P_1 and P_2 related to charge stripes support that the electron-phonon interaction plays an important role in charge ordering in the system.^{30,31}

In summary, we have presented both the resistivity and ultrasonic measurements of LNSCO system. The interaction between dynamic charge stripes and pinning centers was identified by a broad peak around 100 K in elastic energy loss Q^{-1} . With increasing Nd doping level, the activation energy of the disordered charge stripes overcoming the pinning centers increases. For $y \geq 0.3$, associated with the LTO-LTT transition, the dynamic stripes were pinned by the LTT structure and developed to static ones. Strong coupling between the stripes and the ultrasonic provide evidence that electron-phonon interaction plays an important role in charge ordering in cuprates.

ACKNOWLEDGMENTS

This work was supported by the Chinese National Nature Science Fund and the Ministry of Science and Technology of China.

*Author to whom correspondence should be addressed. Electronic address: lixg@ustc.edu.cn

¹For review, see E. W. Carlson, V. J. Emery, S. A. Kivelson, and D. Orgad, cond-mat/0206217 (unpublished).

²J. M. Tranquada, B. J. Sternlieb, J. D. Axe, Y. Nakamura, and S. Uchida, *Nature (London)* **375**, 561 (1995).

³J. M. Tranquada, J. D. Axe, N. Ichikawa, Y. Nakamura, S. Uchida, and B. Nachumi, *Phys. Rev. B* **54**, 7489 (1996).

⁴J. M. Tranquada, J. D. Axe, N. Ichikawa, A. R. Moodenbaugh, Y. Nakamura, and S. Uchida, *Phys. Rev. Lett.* **78**, 338 (1997).

⁵H. A. Mook, P. C. Dai, S. M. Hayden, G. Aeppli, T. G. Perring, and F. Dogan, *Nature (London)* **395**, 580 (1998).

⁶T. Noda, H. Eisaki, and S. Uchida, *Science* **286**, 265 (1999).

⁷S. Arumugam, N. Mori, N. Takeshita, H. Takashima, T. Noda, H. Eisaki, and S. Uchida, *Phys. Rev. Lett.* **88**, 247001 (2002).

⁸K. Yamada, C. H. Lee, K. Kurahashi, J. Wada, S. Wakimoto, S. Ueki, H. Kimura, Y. Endoh, S. Hosoya, G. Shirane, R. J. Birgeneau, M. Greven, M. A. Kastner, and Y. J. Kim, *Phys. Rev. B* **57**, 6165 (1998).

⁹A. W. Hunt, P. M. Singer, K. R. Thurber, and T. Imai, *Phys. Rev. Lett.* **82**, 4300 (1999).

¹⁰Y. Ando, K. Segawa, S. Komiya, and A. N. Lavrov, *Phys. Rev. Lett.* **88**, 137005 (2002).

¹¹F. Cordero, A. Paolone, R. Cantelli, and M. Ferretti, *Phys. Rev. B* **67**, 104508 (2003).

¹²M. Von Zimmermann, A. Vigliante, T. Niemoller, N. Ichikawa, T. Frello, J. Madsen, P. Wochner, S. Uchida, N. H. Andersen, J. M. Tranquada, D. Gibbs, and J. R. Schneider, *Europhys. Lett.* **41**, 629 (1998).

¹³S. Bhattacharya, M. J. Higgins, D. C. Johnston, A. J. Jacobson, J. P. Stokes, J. T. Lewandowski, and D. P. Goshorn, *Phys. Rev. B* **37**, 5901 (1988).

¹⁴M. Nohara, T. Suzuki, Y. Maeno, T. Fujita, I. Tanaka, and H. Kojima, *Phys. Rev. Lett.* **70**, 3447 (1993).

¹⁵Y. N. Huang, Y. N. Wang, and Z. X. Zhao, *Phys. Rev. B* **49**, 1320 (1994).

¹⁶J. Yamada, M. Sera, M. Sato, T. Takayama, M. Takata, and M. Sakata, *J. Phys. Soc. Jpn.* **63**, 2314 (1994).

- ¹⁷M. B. Walker, M. F. Smith, and K. V. Samokhin, *Phys. Rev. B* **65**, 014517 (2001).
- ¹⁸E. S. Bozin, S. J. L. Billinge, G. H. Kwei, and H. Takagi, *Phys. Rev. B* **59**, 4445 (1999).
- ¹⁹A. S. Nowick, and B. S. Berry, *Anelastic Relaxation in Crystalline Solids* (Academic Press, New York, 1972).
- ²⁰A. R. Moodenbaugh, L. H. Lewis, and S. Soman, *Physica C* **290**, 98 (1997).
- ²¹S. Wakimoto, R. J. Birgeneau, Y. Fujimaki, N. Ichikawa, T. Kasuga, Y. J. Kim, K. M. Kojima, S. H. Lee, H. Niko, J. M. Tranquada, S. Uchida, and M. V. Zimmermann, *Phys. Rev. B* **67**, 184419 (2003).
- ²²B. Büchner, M. Breuer, A. Freimuth, and A. P. Kampf, *Phys. Rev. Lett.* **73**, 1841 (1994).
- ²³M. Hücker, V. Kataev, J. Pommer, O. Baberski, W. Schlabitz, and B. Büchner, *J. Phys. Chem. Solids* **59**, 1821 (1998).
- ²⁴V. V. Moshchalkov, J. Vanacken, and L. Trappeniers, *Phys. Rev. B* **64**, 214504 (2001).
- ²⁵M. K. Crawford, R. L. Harlow, E. M. McCarron, W. E. Farneth, J. D. Axe, H. Chou, and Q. Huang, *Phys. Rev. B* **44**, 7749 (1991).
- ²⁶A. R. Moodenbaugh, Lijun Wu, Yimei Zhu, L. H. Lewis, and D. E. Cox, *Phys. Rev. B* **58**, 9549 (1998).
- ²⁷J. M. Tranquada, N. Ichikawa, and S. Uchida, *Phys. Rev. B* **59**, 14 712 (1999).
- ²⁸F. C. Chou and D. C. Johnston, *Phys. Rev. B* **54**, 572 (1996).
- ²⁹F. Cordero, C. R. Grandini, G. Cannelli, R. Cantelli, F. Trequattrini, and M. Ferretti, *Phys. Rev. B* **57**, 8580 (1998).
- ³⁰A. Lanzara, G. M. Zhao, N. L. Saini, A. Bianconi, K. Conder, H. Keller, and K. A. Müller, *J. Phys.: Condens. Matter* **11**, L541 (1999).
- ³¹G. M. Zhao, *Philos. Mag. B* **81**, 1335 (2001).